2013-09-01

Analysis of the Thermal Performance of a Solar Water Heating System with Flat Plate Collectors in a Temperate Climate

Lacour Ayompe
Dublin Institute of Technology, lacour.ayompe@dit.ie

Aidan Duffy
Dublin Institute of Technology, aidan.duffy@dit.ie

Recommended Citation

Ayompe, L. and Duffy, A. Analysis of the thermal performance of a solar water heating system with flat plate collectors in a temperate climate. Applied Thermal Engineering (2013): 58; 447-454. doi:10.1016/j.applthermaleng.2013.04.062

Analysis of the thermal performance of a solar water heating system with flat plate collectors in a temperate climate

L.M. Ayompe[1] and A. Duffy
School of Civil & Building Services Engineering and Dublin Energy Lab, Dublin Institute of Technology, Dublin 1, Ireland.

Abstract

The thermal performance of a solar water heating system with 4 m^2 flat plate collectors in Dublin, Ireland is presented in this paper. The experimental setup consisted of a commercially available forced circulation domestic scale system fitted with an automated sub-system that controlled hot water draw-offs and the operation of an auxiliary immersion heater. The system was tested over a year and the maximum recorded collector outlet fluid temperature was 70.4 ^oC while the maximum water temperature at the bottom of the hot water tank was 59.9 ^oC. The annual average daily energy collected was 19.6 MJ/d, energy delivered by the solar coil was 16.2 MJ/d, supply pipe loss was 3.2 MJ/d, solar fraction was 32.2%, collector efficiency was 45.6% and system efficiency was 37.8%. Supply pipe losses represented 16.4% of energy collected.

Keywords: Solar water heating system, flat plate collector, solar controller, temperate climate

1. Introduction

A glazed flat plate collector (FPC) consists of a metal absorber in a flat rectangular casing. A glass cover on the upper surface and insulation at the bottom and sides reduce thermal losses. Air is present in the space between the metal absorber and transparent cover. The flat metal plate serves as a heat exchanger that absorbs solar radiation, converts it into heat and transfers the heat to a flowing fluid. The heat can be used directly if water is

[1] Corresponding author: Email address: lacour.ayompe@dit.ie (L.M. Ayompe); Tel: +353 14027937

used as the transfer fluid or transferred to water in a storage tank using a heat exchanger if a solar fluid is used [1].

The annual average efficiency of well designed solar water heating systems (SWHSs) with FPCs in northern temperate climates is typically around 35-40% [2]. Temperate climates are those without temperature extremes and precipitation (rain and snow) with changes between summer and winter being generally refreshing without being frustratingly extreme. A temperate weather however, can have a very changeable weather in both summer and winter. One day it may be raining, the next it may be sunny. These climates are located in zones in the range of latitudes between 40 and 60/70^{o} North [3].

Solar energy collectors are the main component of SWHSs therefore evaluating their thermal performance is vital. A number of studies on the performance of FPCs have been carried out under steady-state and quasi-dynamic test conditions following EN 12975-2 [4] and ASHRAE 93-86 [5] standards. Zambolin and Del Col [6] carried out a comparative performance analysis of the thermal performance of flat plate and evacuated tube collectors in Padova, Italy. They presented a new set of data collected for both flat plate and evacuated tube collectors tested simultaneously from steady-state and quasi-dynamic efficiency tests following the standard EN 12975-2.

Tiwari et al. [7] analysed the performance of solar FPCs manufactured in India with F_RU_L values ranging between 5.139 and 7.024. Amer et al. [8] developed a transient method to characterise the dynamic behaviour of solar FPCs and validated their results for $F(\tau\alpha)_e$ and FU_L against those obtained from steady state tests based on the ASHRAE 93-86 standard. They also investigated the effects of inlet temperature and incidence alngle on collector parameters. Chen et al. [9] carried out tests to evaluate the efficiencies of two solar FPCs at different flow rates. Sakhrieh and Al-Ghandoor [10] conducted an experimental study to characterise the overall performance of four types of FPCs and an evacuated tube collector used in Jordan.

Data obtained from these tests are used to characterise collectors using efficiency curves. However, these test conditions do not represent typical weather and operating conditions under which SWHSs are subjected to. Consequently, other studies have focused on evaluating the performance of SWHSs under real weather conditions. Rodríguez-Hidalgo et al. [11] studied the performance of a 50 m^2 solar FPC array for domestic hot water heating and cooling applications in Madrid, Spain.

Michaelides and Eleftheriou [12] studied the behaviour of a SWHS with 3 m^2 FPC and a 68 L hot water tank in Cyprus using data collected over 2 years. Ayompe et al. [13] compared the year round energy and economic performance of two SWHSs with flat plate and evacuated tube collectors operating under the same weather conditions in Dublin, Ireland. Building Research Establishment [14] evaluated the performance of a SWHS in Cambridgeshire, UK which had a flat plate solar panel (Clearline V30) manufactured by Viridan Solar, UK. The test rig included an automated system that incorporated the effects of the auxiliary heating system (boiler or immersion heater) and daily hot water use of the average European household described by the EU reference tapping cycle (EU M324EN) equivalent to 100 litres at 60°C. Their results showed that over a year, the 3 m^2 collector generated 5,266 MJ of heat accounting for 57% of the hot water requirement.

This paper presents results on the analysis of the thermal performance of a SWHS with 4 m^2 FPCs using data from a field trial in Dublin, Ireland. The SWHS is typical of systems installed in average sized single domestic dwellings in Ireland with 4-6 inhabitants. An automated sub-system was developed to control hot water draw-offs to mimic the demand for hot water in domestic dwellings. An electric immersion heater was used to provide 'top-up' energy when insufficient solar radiation was available, as is typical in Ireland and the UK. The data collected were used to evaluate energy performance indices notably: system component temperatures, collector energy outputs; energy delivered to the hot water tank;

collector and system efficiencies; pipework heat loss; and solar fraction on daily, monthly and yearly basis.

2. Methodology

A forced circulation SWHS with 4 m^2 FPC was installed on a flat rooftop in the Focas Institute, Dublin, Ireland (latitude 53°20' N and longitude 6°15') and its thermal performance was monitored over a one year period. The SWHS had a 300 litre hot water tank equipped with an electrical auxiliary immersion heater which was used to top up the tank temperature to 60^{o}C in the morning and evening whenever the solar coil fell short of doing so. An automated hot water draw off system was developed to mimic domestic hot water use (volumetric flow rates are shown in Fig. 1). System performance data were collected every minute.

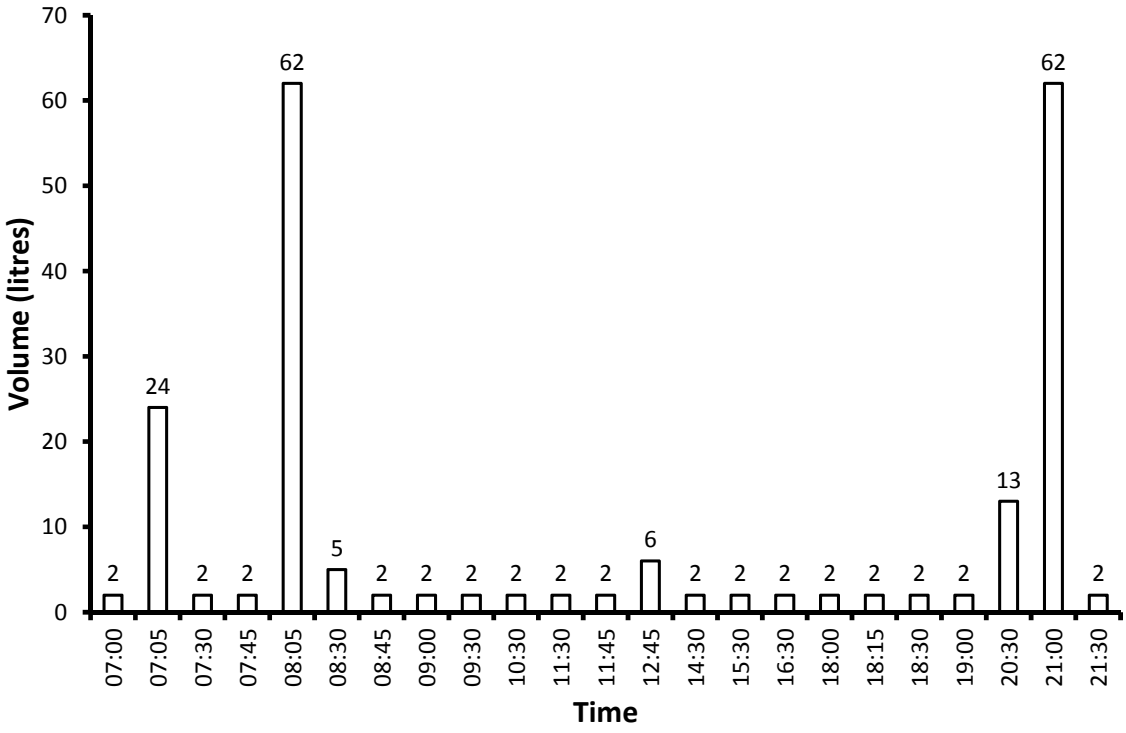

Fig. 1. Volume of hot water (60^{o}C) draw-off at different times of the day.

2.1. System description

Typical solar water heating systems used in temperate climates consist of a hot water storage tank, control unit, pump station and either flat plate or evacuated tube collectors. The FPC employed in this study was south facing and inclined at 53^{o}, equal to the local latitude of the location. The hot water tank was installed nearby in the building's plant room. The solar circuits consisted of 12 mm diameter (outside) copper pipes insulated with 22 mm thick Class O Armaflex. All pipe fittings were insulated to reduce heat losses. The solar circuit pipe length supply and return were 14 m and 15.4 m respectively.

The collecting sub-system consisted of two K420-EM2L flat plate collectors each with a gross area of 2.18 m^2 and aperture area of 2 m^2 connected in series giving a total area of 4 m^2. The absorber material consisted of aluminium coated with eta plus (a highly selective coating with 95% absorbance and 5% emittance). The collectors each had a single transparent cover made up of tempered solar safety glass. The collectors were insulated with 30 mm thick mineral wool. Each collector had maximum operating and stagnation temperatures of 120 ^{o}C and 191 ^{o}C respectively, a maximum operating pressure of 10 bar and a fluid content of 1.73 l.

The stainless steel hot water tank (model HM 300L D/coil U44332) was 1,680 mm high with a diameter of 580 mm and an operating pressure of 3 bar. The tank was equipped with an electric immersion heater of 2.75/3.0 kW capacity located at the middle of the tank. The tank had a heating coil with surface area of 1.4 m^2 and a rating of 21 kW.

The hot water demand profile employed was the EU reference tapping cycle number 3 (see Fig. 1), equivalent to a daily energy output of 42.1 MJ representing 199.8 litres of water at 60^{o}C. It is based on hot water use of the average European household described in

the European Union mandate for the elaboration and adoption of measurement standards for household appliances EU M324EN [15].

An automated hot water dispensing unit was designed and incorporated into the SWHS to draw-off water from the hot water tank in such a way as to mimic real life operation by households. The unit includes a programmable logic controller (PLC), contactors, relays, electrical fittings, solenoid valve, thermostat and impulse flow meters. A software program was written to control the auxiliary heating system as well as opening and shutting the solenoid valves.

Fig. 2 shows a flow chart of the daily operation of the PLC. The PLC turned on the immersion heater at the middle of the hot water tank between 5-8 am and 6-9 pm daily just before the two peak hot water draw-offs to ensure that hot water was available when needed. An analogue thermostat placed at the top of the hot water tank was set to turn off the electricity supply to the immersion heater when the temperature of the water at the top of the tank exceeded 60^{o}C. Hot water was dispensed using a solenoid valve that was opened and closed using signals from the PLC. A pulse flow meter (1 pulse per litre) installed at the end of the solenoid valve was used to count the number of litres of water extracted from the hot water tank. The solenoid valve was closed when the required volume of water was dispensed based on the water demand profile (see Fig. 1).

Fig. 3 shows a schematic diagram of the experimental setup of the SWHS components and the position of the thermocouple sensors. Parameters measured include the following: solar fluid temperature at the collector outlet (Tc,o), water temperature at the bottom of the hot water tank (Tb,t), water temperature at the middle of the hot water tank (Tm,t), solar fluid temperature at inlet to the solar coil (Tsc,i), solar fluid temperature at the outlet from the solar coil (Tsc,o), solar fluid temperature at inlet to the collector (Tc,i),

cold water inlet temperature to the hot water tank (Tcw,i), hot water supply temperature (Thw,o) and the volume flow rate of the solar fluid.

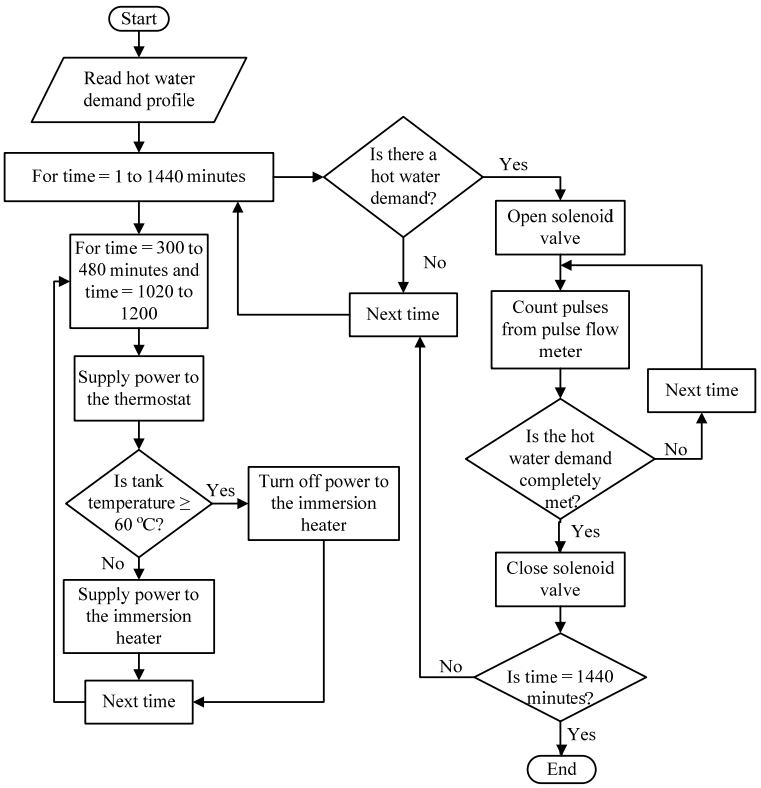

Fig. 2. Flow chart of the daily operation of the PLC

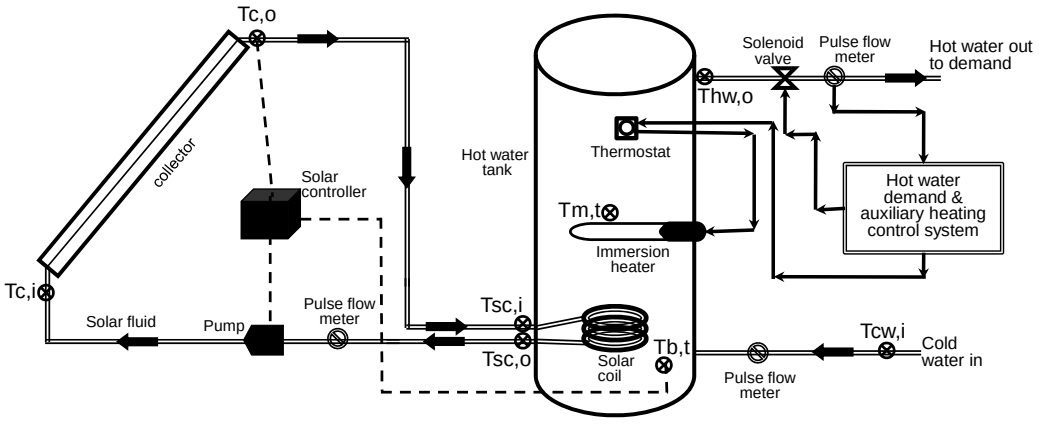

Fig. 3. Schematic diagram of the experimental setup.

2.2 Data measurement and logging

The SWHS was equipped with a RESOL DeltaSol M solar controller which had relay inputs to control the operation of the solar pump station. It also had temperature sensor inputs onto which PT1000 platinum resistance temperature sensors were connected to measure water and solar fluid temperatures (Tc,o-Thw,o) shown in Fig. 3. The volumetric flow rate of the solar fluid was measured using RESOL V40-06 impulse flow meters which react at 1 litre per pulse. RESOL DL2 data loggers were used to store data every minute from the RESOL DeltaSol M solar controllers via RESOL VBus cables. DL2 data loggers were equipped with a secure digital (SD) drive and a local area network (LAN) port for direct connection to a personal computer (PC). Data from the loggers was extracted using a Web browser or an SD card and then converted to text format using the RESOL Service Centre Software.

Global solar radiation on the collector's surface, ambient temperature and wind speed data were measured using a weather station consisting of an SMA Sunny Sensor Box equipped with an ambient temperature sensor and an anemometer. The solar radiation sensor had an accuracy of ±8% and a resolution of 1 W/m^2. The PT1000 platinum temperature sensors had an accuracy of ±0.5 ^oC while the ambient temperature sensor was a JUMO PT 100 U type with accuracy of ±0.5 ^oC. The anemometer was a Thies small wind transmitter with accuracy of ±5%. Weather data was logged at 5 minute intervals using a Sunny Box WebBox.

3. Energy performance analysis

The energy performance indices evaluated in this study include: energy collected, energy delivered and supply pipe losses, solar fraction, collector efficiency and system efficiency.

3.1. *Energy collected*

The useful energy collected by the solar energy collector is given as [16]:

$$Q_c = \dot{m}C_p(Tc,o - Tc,i) \quad (1)$$

3.2. *Energy delivered and supply pipe losses*

The useful energy delivered by the solar coil to the hot water tank is given as

$$Q_d = \dot{m}C_p(Tsc,i - Tsc,o) \quad (2)$$

Supply pipe losses were due to the temperature drop as the solar fluid flowed between the collector outlet and the solar coil inlet to the hot water tank. These losses were calculated as:

$$Q_L = \dot{m}C_p(Tsc,i - Tsc,i) \quad (3)$$

3.3. *Solar fraction*

The solar fraction (SF) is the ratio of solar heat yield to the total energy requirement for water heating and is given as [2]:

$$SF = \frac{Q_s}{Q_s + Q_{aux}} \quad (4)$$

3.4. *Collector efficiency*

The collector efficiency was calculated as [17, 18]:

$$\eta_c = \frac{\dot{m}C_p(Tc,o - Tc,i)}{A_c G_t} \quad (5)$$

3.5. *System efficiency*

The system efficiency was calculated as [17, 18]:

$$\eta_s = \frac{\dot{m}C_p(Tsc,i - Tsc,o)}{A_c G_t} \quad (6)$$

4. Results and discussions

4.1. Daily performance

Three days representative of typical weather conditions prevalent in Ireland were used to analyse the daily performance of the FPC SWHS. They consist of heavily overcast sky (04/02/2010), clear sky (24/05/2009) and intermittent cloud covered sky (13/10/2009). Fig. 4 shows plots of solar radiation during the three days. The maximum daily solar radiation was 176.3 W/m^2 on the heavily overcast day, 961.8 W/m^2 on the clear sky day and 633.4 W/m^2 on the day with intermittent cloud cover. Fig. 5 shows plots of ambient air temperature and wind speed. The maximum ambient air temperatures and wind speeds were: 10.5 ^{o}C and 8.7 m/s on the heavily overcast day; 21.8 ^{o}C and 9.1 m/s on the clear sky day; 18.6 ^{o}C and 3.4 m/s on the day with intermittent cloud cover.

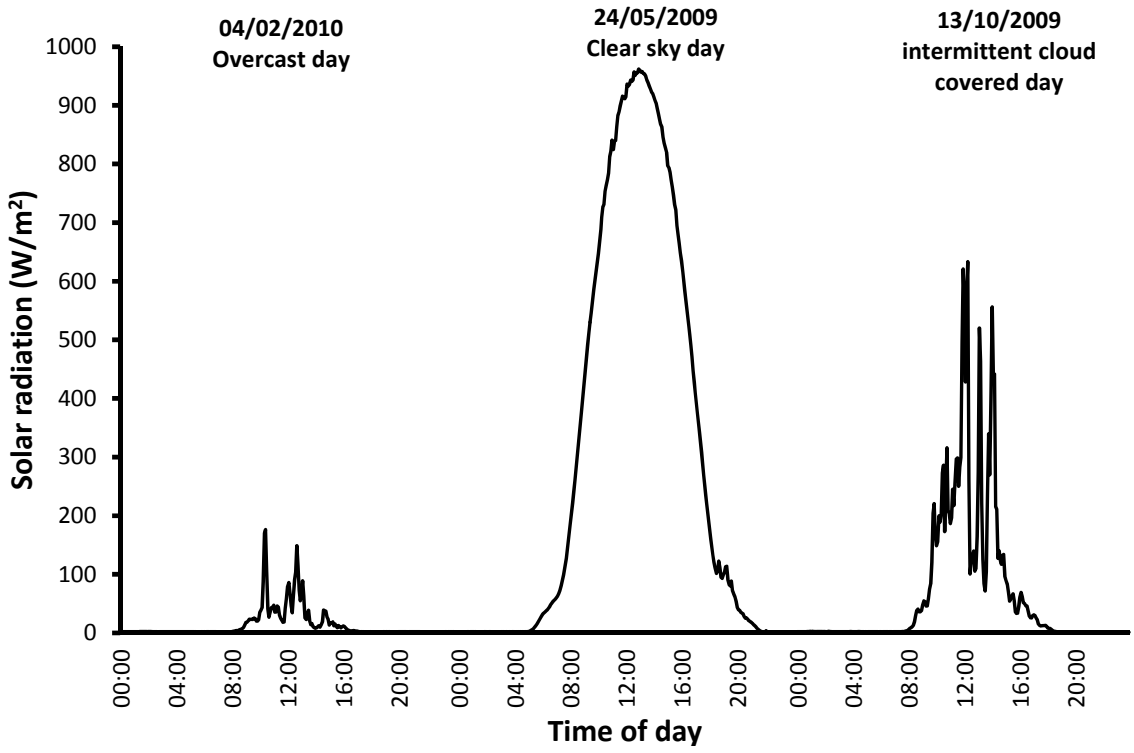

Fig. 4. Global solar radiation on the collector surface for three characteristic days

4.1.1 System temperatures

Fig. 6 shows plots of daily variation in solar fluid temperature at the collector's outlet (Tc,o), water temperature at the bottom of the hot water tank (Tb,t), cold water inlet temperature to the hot water tank (Tcw,i). It is seen that a rise in Tc,o due to solar gain through the collector causes a delayed increase in Tb,t. The time lag is caused by the time it takes for heat exchange between the solar fluid and water in the tank as well as conduction through the tank fluid to the sensor Tb,t. Cold water supply was from a tank located in the boiler room of the building on which the experimental rig was installed. Short term variations in Tcw,i were as a result of changes in water temperature in the boiler room where the hot water tank was installed.

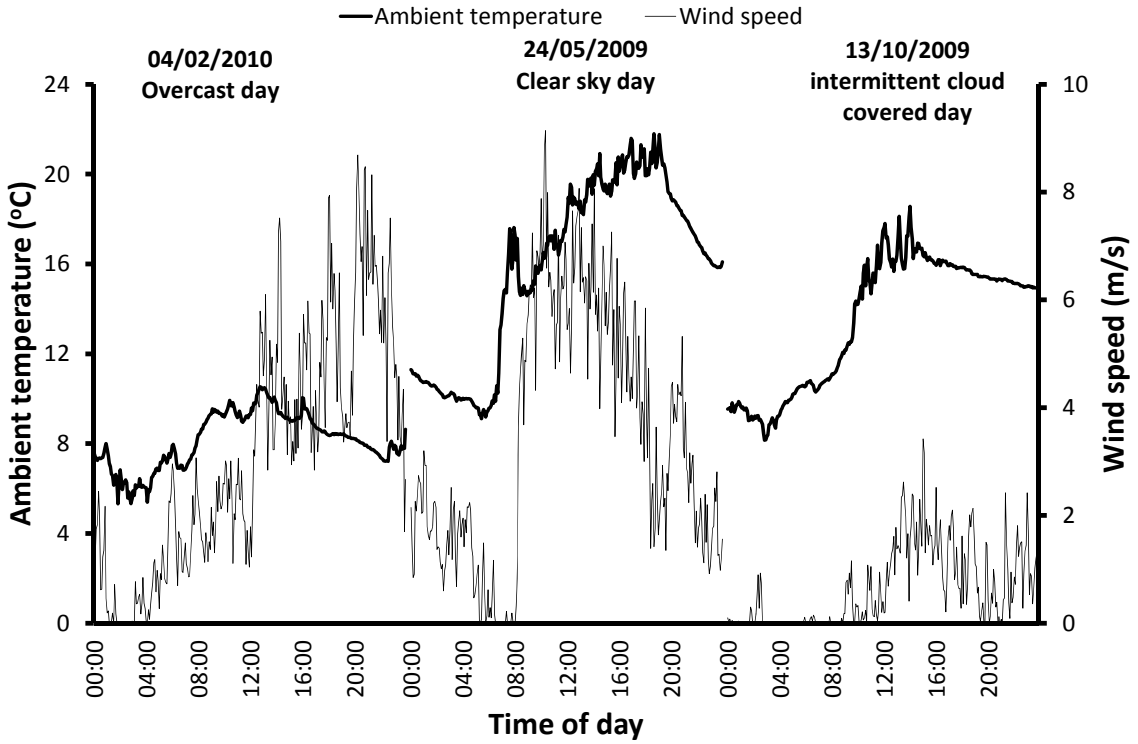

Fig. 5. Ambient air temperature and wind speed for three characteristic days.

Fig. 7 shows plots of daily variation of solar fluid temperature at the collector outlet (Tc,o), water temperature at the bottom of the hot water tank (Tb,t) and water temperature at the middle of the hot water tank (Tm,t). It is seen that a rise in Tc,o causes an increase in

both Tb,t and Tm,t with both of them lagging behind Tc,o for the same reason explained above. During the heavily overcast and intermittent cloud covered sky days, the immersion heater is called on twice (in the morning and evening) while it is called up only in the morning during the clear sky day since the solar coil raises the water temperature in the tank to the desired level during the daytime period. Tb,t and Tm,t remained very close throughout the heating period with the solar coil during the clear sky day.

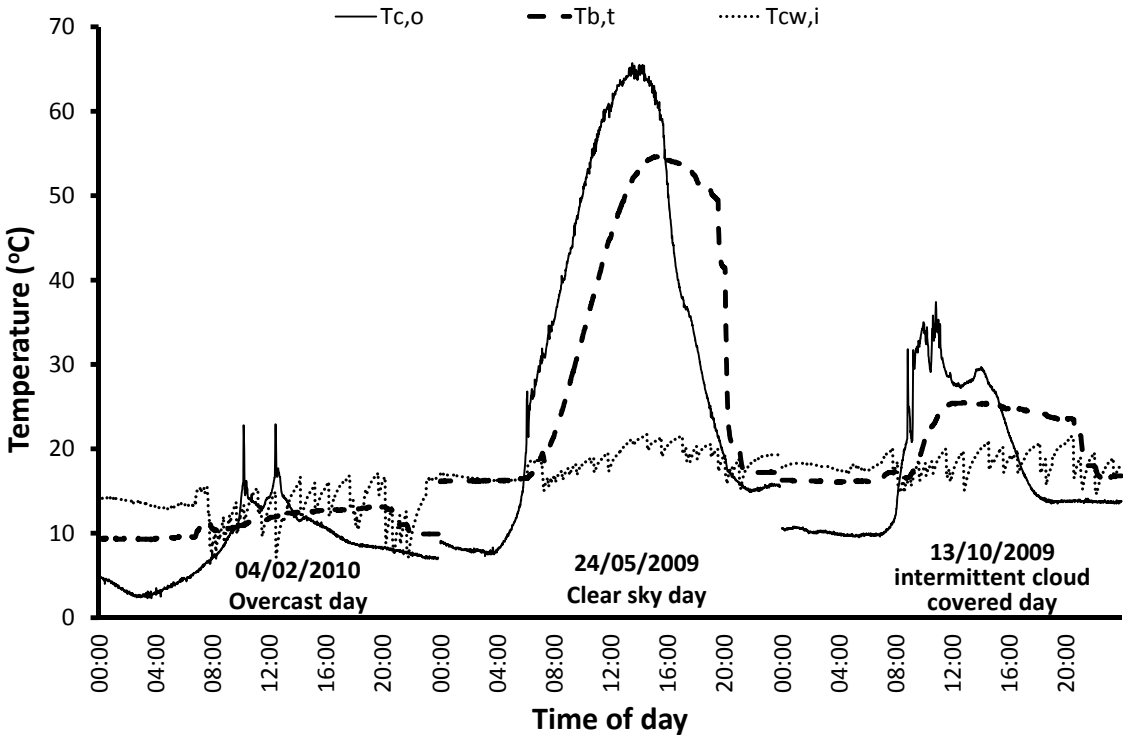

Fig. 6. Daily variation of Tc,o, Tb,t and Tcw,i.

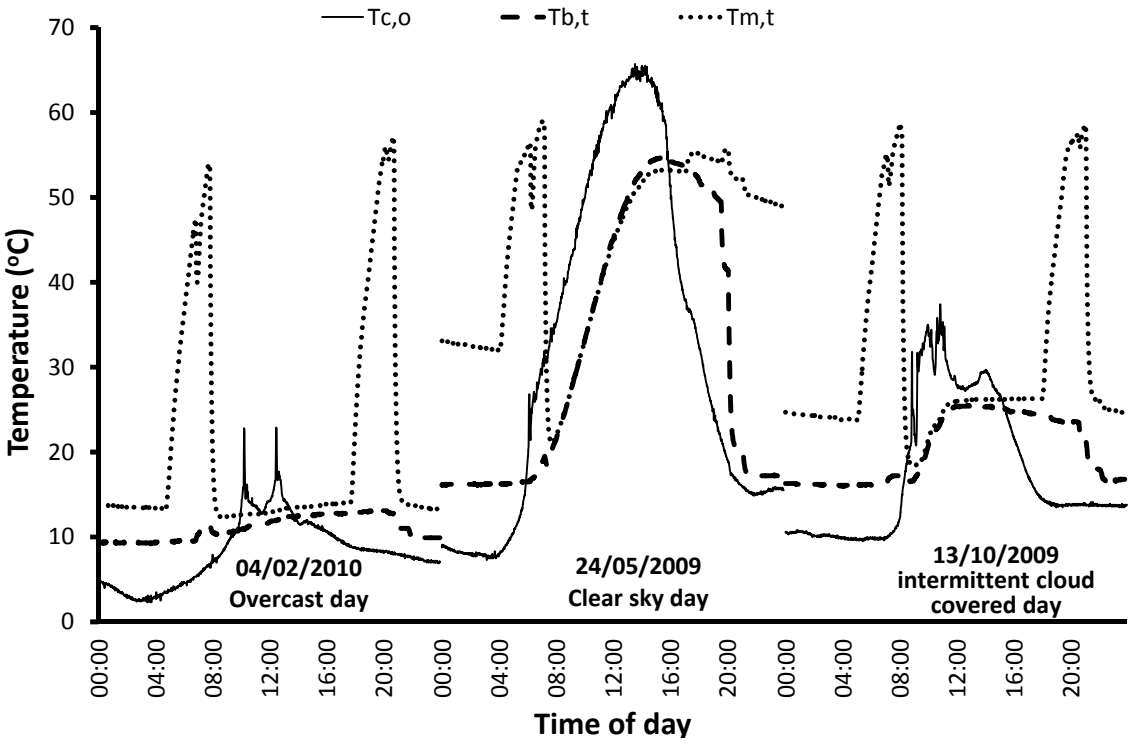

Fig. 7. Daily variation of Tc,o, Tb,t and Tm,t.

Fig. 8 shows plots of daily variation of water temperature at the bottom of the hot water tank (Tb,t), water temperature at the middle of the hot water tank (Tm,t) and hot water supply temperature (Thw,o). Due to difficulties in inserting the thermocouples at the top of the hot water tank, the water temperatures at the top of the tank were considered to be the same as the maximum values of Thw,o measured during hot water draw-offs. It is seen that during heavily overcast days, Thw,o drops to about 30 ^{o}C as water is continuously withdrawn from the tank using the tapping cycle. However, during the clear sky day, Thw,o did not drop below 50^{o}C due to the relatively greater quantity of heat delivered by the solar coil throughout the day time. This shows that for a continuous stream of clear sky days, the SWHS would provide all the hot water required in the evening with a reduced quantity of auxiliary energy required in the morning.

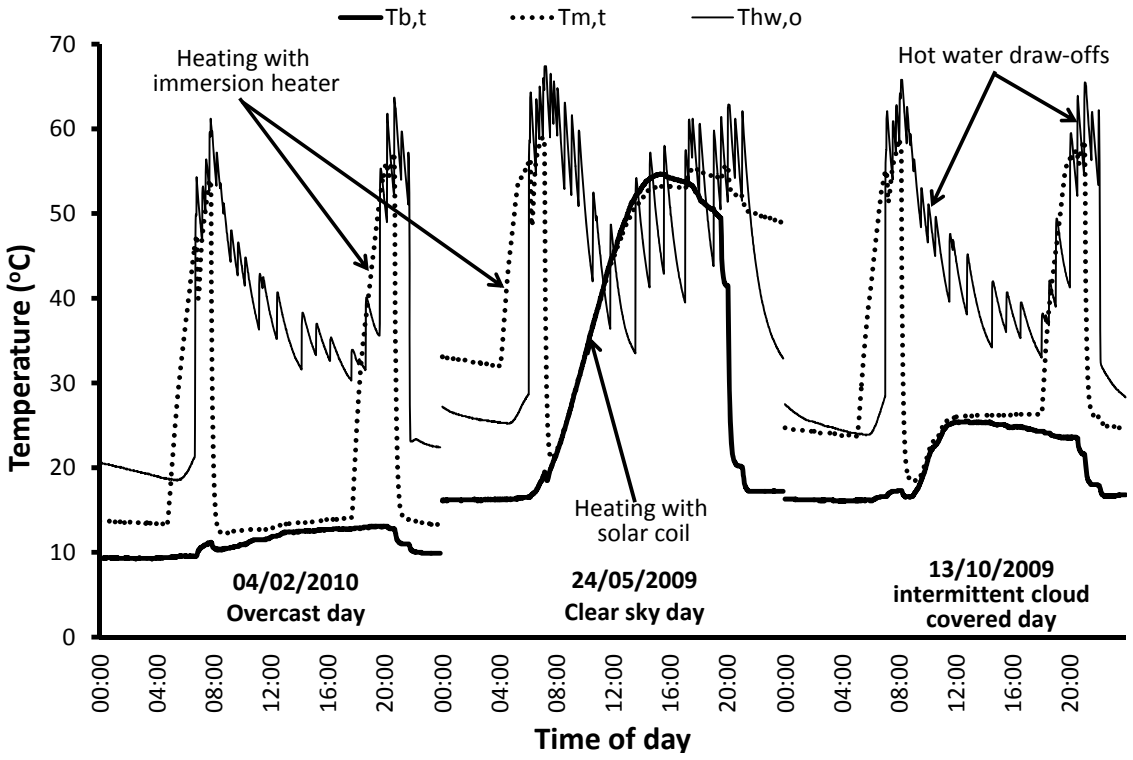

Fig. 8. Daily variation of Tb,t, Tm,t and Thw,o.

The immersion heater at the middle of the tank was programmed to switch on between 5-8 am and 6-9 pm daily. An analogue thermostat installed at the top of the tank was used to maintain the water temperature around 60 ^{o}C. This ensured that hot water was available in the tank when needed to satisfy the largest hot water demands at 7:05 am, 8:05 am, 8:30 pm and 9:00 pm as shown in Fig. 1. The timing was such that there was always enough cold water at the bottom of the hot water tank to be heated by the solar coil during even on a clear sky day (24/05/2009) when no auxiliary energy was required from the immersion heater in the evening. On the other hand, during a heavily overcast day (04/02/2010) or intermittent cloud covered day (13/10/2009) the immersion heater was used to heat water in the tank both in the morning and evening.

4.1.2. Solar fluid mass flow rate

Fig. 9 shows variation of the solar fluid mass flow rate during the three days. On the heavily overcast day the pump came on only twice for very short intervals running at 0.047,

0.062 and 0.092 kg/s. During the clear sky and intermittent cloud covered days the pump operated at six different flow rates 0.047, 0.062, 0.092, 0.111, 0.130 and 0.149 kg/s depending on the intensity of solar radiation. On the clear sky day the flow rates during solar noon were 0.130 and 0.149 kg/s. Table 1 shows the percentage of time the SWHS pump operated at different flow rates.

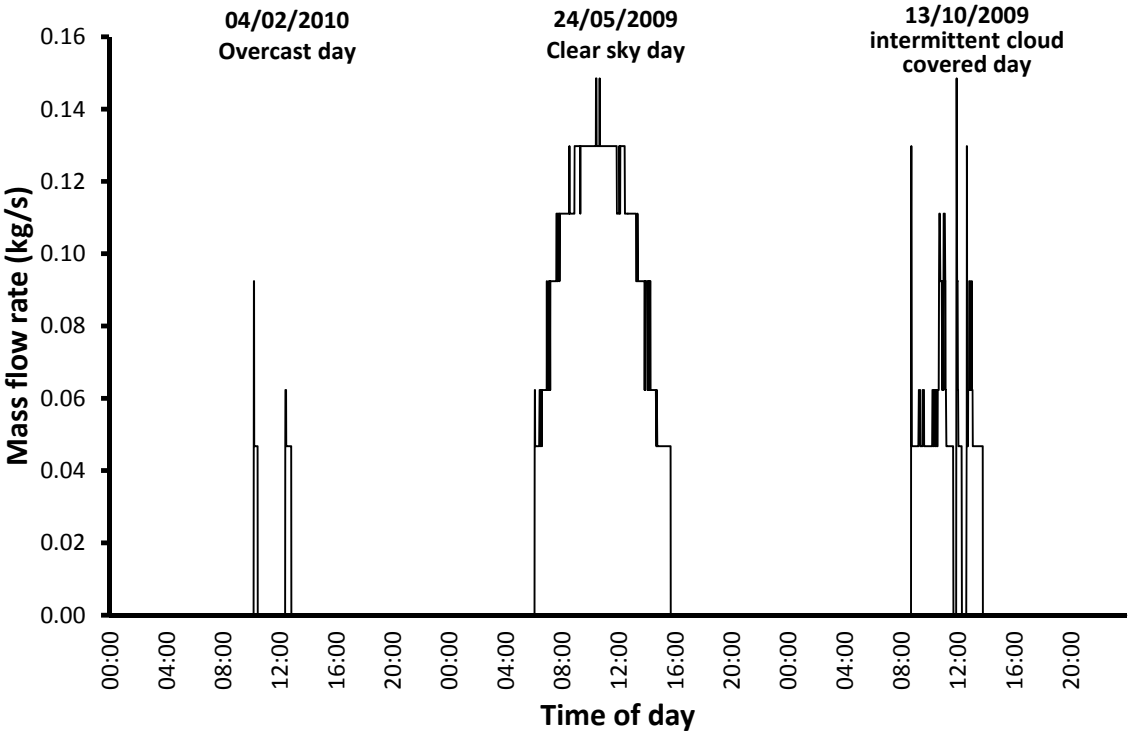

Fig. 9. Solar fluid mass flow rate.

Table 1: Percentage of time the SWHS pump operated at different flow rates

	Percentage (%)		
Flow rate (kgs^{-1})	Heavily overcast day (04/02/2010)	Clear sky day (24/05/2009)	Intermittent cloud covered day (13/10/2009)
0.047	88.4	14.4	66.1
0.062	7.0	13.1	19.2
0.092	4.7	14.5	8.5
0.111	0.0	23.2	5.2
0.130	0.0	34.3	0.7
0.149	0.0	0.5	0.4

4.1.3. Energy collected

Fig. 10 shows the energy collected by the FPC system. The total daily energy collected was 209.7 MJ on 04/02/2010, 7,294.3 MJ on 24/05/2009 and 1,649.6 MJ on 13/10/2009. Fig. 11 shows a scattered plot of the daily energy collected against solar energy input. It is seen that the daily energy collected by the FPCs has a linear relationship with daily solar energy input with correlation coefficient (R^2) of 0.9439. The high correlation coefficient shows that the daily energy collected by the FPCs can be predicted for any given day known total daily solar energy using equation 7 given as:

$$E_c = 0.4847E_i - 0.3845 \quad (7)$$

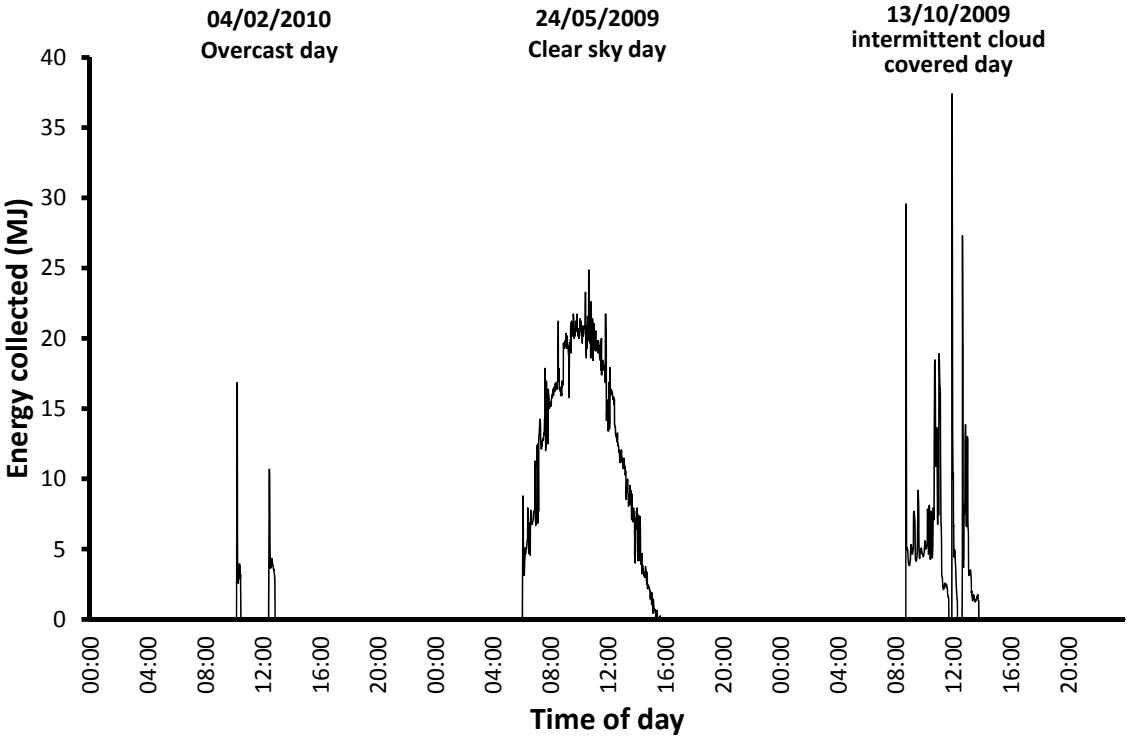

Fig. 10. Energy collected.

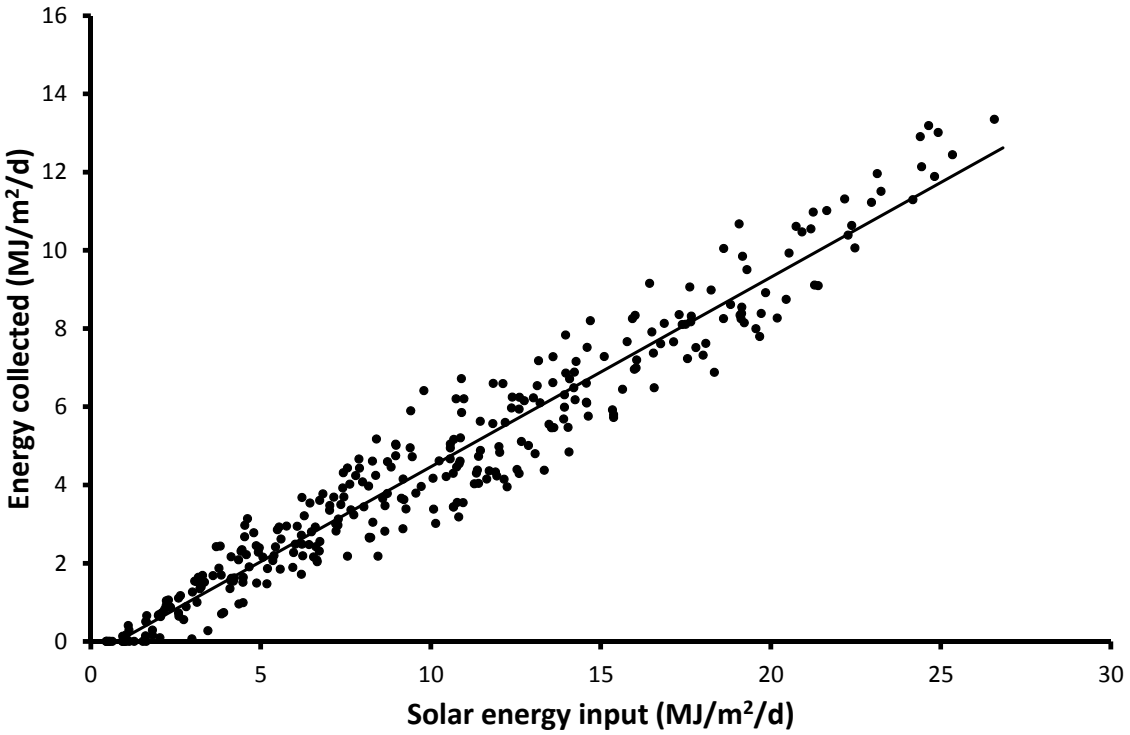

Fig. 11. Daily energy collected against solar energy input.

4.2. Monthly Performance

4.2.1. System temperatures

Fig. 12 shows maximum recorded monthly water temperatures at Tc,o, Tb,t, Tm,t, Tcw,i and Thw,o. The maximum monthly water temperatures at Tm,t and Thw,o were fairly constant throughout the year around 60.0 ^{o}C and 68.0 ^{o}C. Maximum monthly fluid temperatures at Tc,o varied between 42.9 ^{o}C in December and 70.4 ^{o}C in June, Tb,t varied between 25.3 ^{o}C in December and 59.9 ^{o}C in June while Tcw,i varied between 17.6 ^{o}C in March and 28.0 ^{o}C in June.

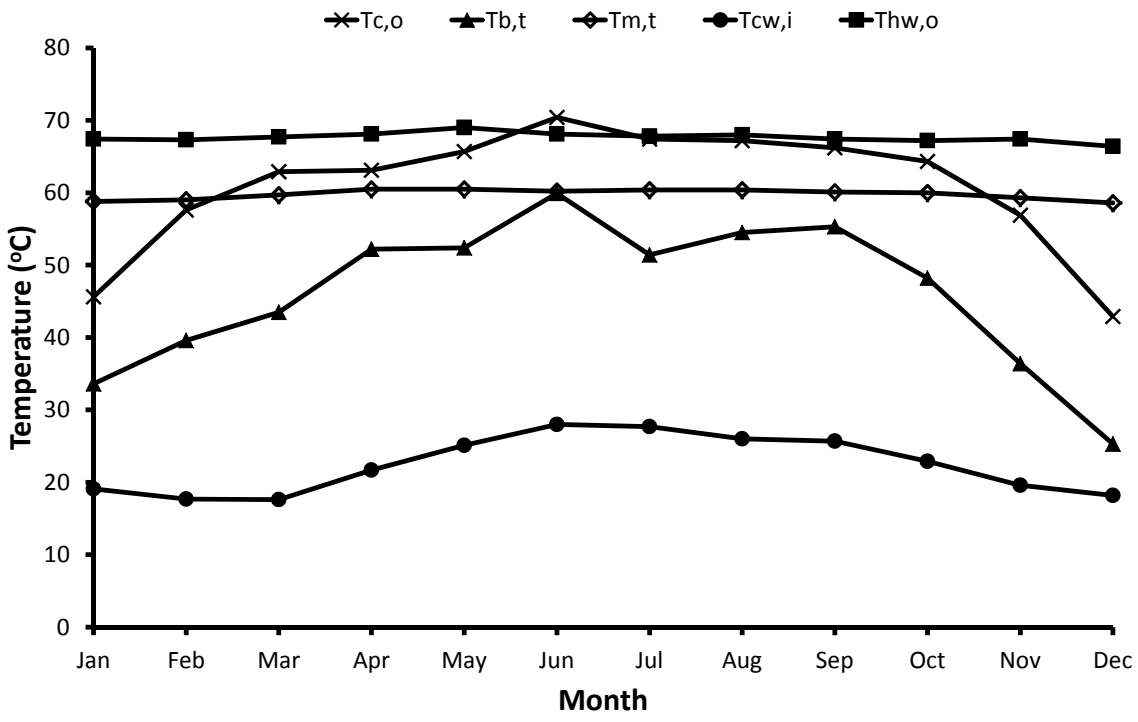

Fig. 12. Maximum monthly water temperatures at Tc,o, Tb,t, Tm,t, Tcw,i and Thw,o.

4.2.2. Energy collected, delivered and losses

Fig. 13 shows monthly and annual average daily global solar insolation on the collector's surface, energy collected and delivered to the hot water tank as well as supply pipe losses. The monthly average daily global solar insolation on the collector's surface varied between 17.3 MJ/d in December and 66.2 MJ/d in June, energy collected varied between 7.2 MJ/d in December and 33.1 MJ/d in April, energy delivered varied between 5.8 MJ/d in December and 27.0 MJ/d in April while supply pipe losses varied between 1.4 MJ/d in December and 5.0 MJ/d in April. Annual average daily solar insolation on the collector's surface was 43.0 MJ/d, energy collected was 19.6 MJ/d, energy delivered was 16.2 MJ/d and supply pipe loss was 3.2 MJ/d.

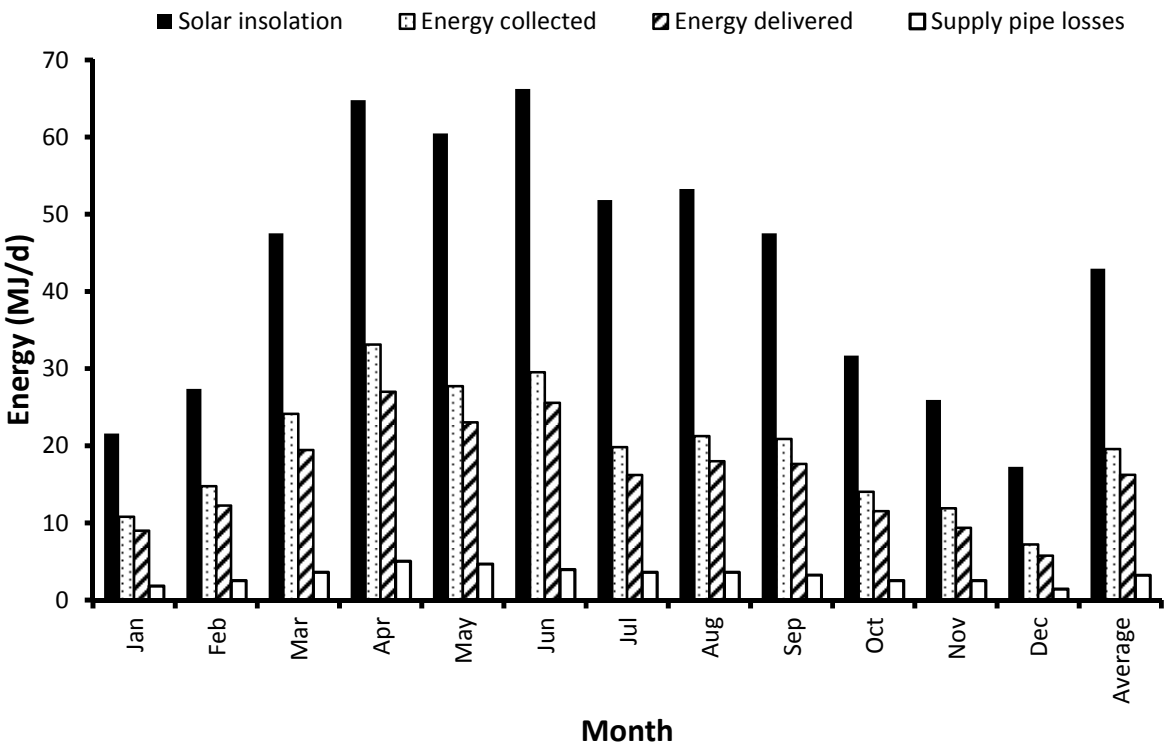

Fig. 13. Monthly and annual average daily global solar insolation on the collector's surface, energy collected, delivered and supply pipe losses.

For an annual global solar insolation on the collector's surface of 15,680.4 MJ, a total of 7,150.4 MJ was collected while 5,924.0 MJ was delivered to the hot water tank. Heat losses along the supply side of the solar circuit occurred especially at high collector outlet temperatures. The total annual supply pipe heat loss for the SWHS was 1,171.7 MJ corresponding to 16.4% of energy collected by the FPC and 19.8% of energy delivered to the hot water tank. The supply pipe length should therefore be kept as short as possible and all joints insulated to reduce heat losses. However, this was not the case for our test rig since the hot water tank was located inside the boiler room of the building on which the FPC was installed.

4.2.3. Energy extracted, auxiliary energy and solar fraction

Fig. 14 shows monthly average daily and annual average energy delivered to the hot water tank, auxiliary energy supplied by the electric immersion to the hot water tank and

solar fraction. The monthly average daily and annual average energy extracted from the hot water tank is the sum of the energy delivered and the auxiliary energy supplied. The monthly average daily energy extracted varied between 43.2 MJ/d in March and 53.6 MJ/d in May and July. The auxiliary energy varied from 23.8 MJ/d in March to 42.5 MJ/d in December. The solar fraction varied between 11.9% in December and 52.4% in April. The annual average daily energy extracted was 50.3 MJ/d, auxiliary energy was 34.1 MJ/d and solar fraction was 32.2%.

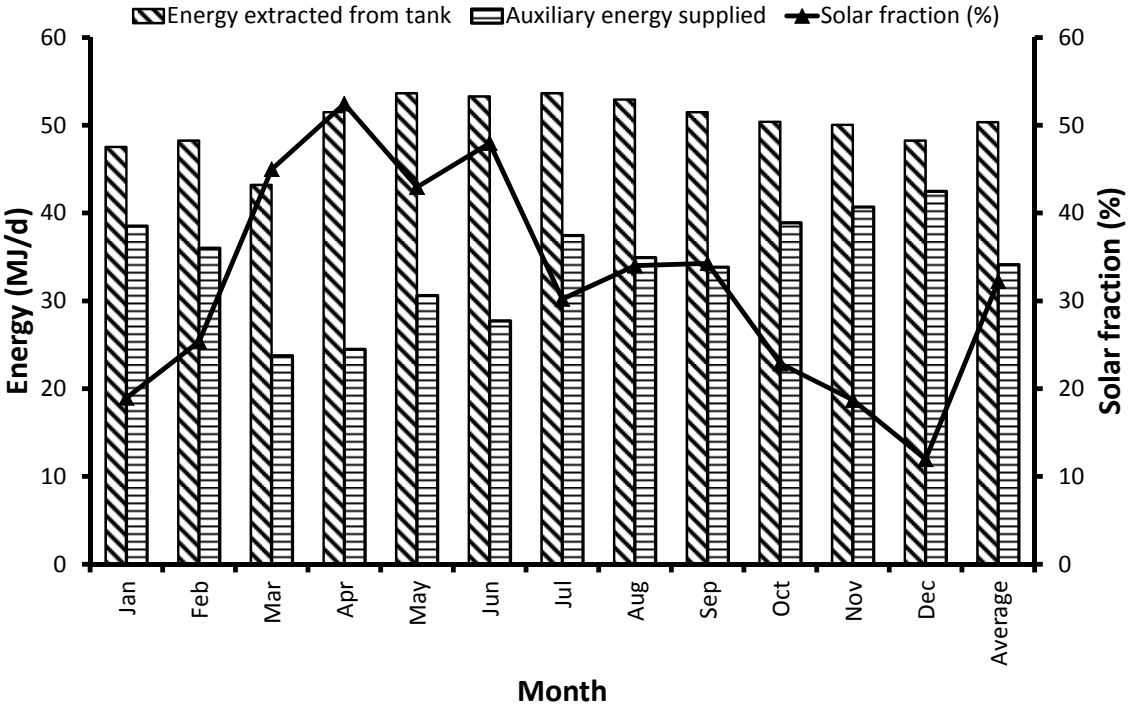

Fig. 14. Energy delivered auxiliary energy and solar fraction.

4.2.4. Collector and system efficiency

Fig. 15 shows monthly average daily collector and system efficiencies. The average daily collector efficiency varied from 38.2% in July to 53.9% in February while the system efficiency varied from 31.3% in December to 44.7% in February. The annual average daily collector efficiency was 45.6% while the system efficiency was 37.8%.

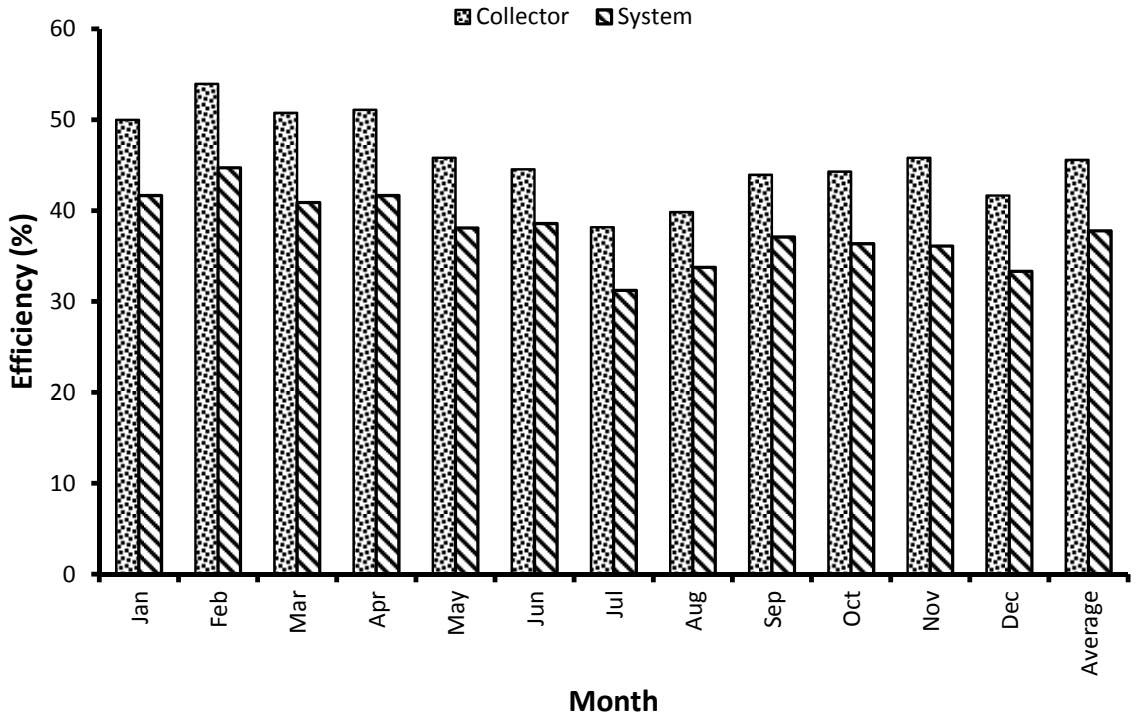

Fig. 15. Monthly average daily collector and system efficiencies.

Using the uncertainties of the measuring instruments presented in section 2.2 and the methods outlined in Mathioulakis et al. [19] and Bell [20], the combined standard uncertainty for measured efficiency and energy collected were calculated as 5.7% and 2.0% respectively. The expanded uncertainty for a 95% level of confidence assuming that the combined uncertainty is normally distributed is 11.4% for measured efficiency and 4.0% for energy collected.

5. Conclusions

The year-round energy performance analysis of a commonly installed SWHS with FPC in a temperate climate was carried out using a field trial installation in Dublin, Ireland. The SWHS was designed and operated to mimic real life operation taking into consideration interaction between the FPC, storage tank and users. An immersion heater was used to

supply auxiliary energy when the solar coil was unable to raise the tank water temperature to the required temperature.

Results showed that for an annual global solar insolation on the collector surface of 15,680.4 MJ, a total of 7,150.4 MJ was collected while 5,924.0 MJ was delivered to the hot water tank. For 12,446.5 MJ of auxiliary energy supplied to meet the total hot water demand of 18,359.5 MJ, the annual solar fraction was 32.2%. Annual average daily energy collected, energy delivered by the solar coil, supply pipe losses were 19.6 MJ/d, 16.2 MJ/d and 3.2 MJ/d respectively. Annual average solar fraction, collector efficiency and system efficiency were 32.2%, 45.6% and 37.8% respectively. The maximum recorded collector fluid outlet temperature was 70.4 ^{o}C while the maximum recorded water temperature at the bottom of the hot water tank was 59.9 ^{o}C.

The total annual supply pipe heat loss for the SWHS was 1,171.7 MJ corresponding to 16.4% of energy collected by the FPC and 19.8% of energy delivered to the hot water tank. The solar circuit supply pipes should therefore be kept as short as possible in order to reduce energy loss. Results from this study and those from the study carried out by Building Research Establishment (2009) revealed that SWHSs with FPCs would generate between 1,750 and 1,790 MJ/m^2/yr of heat in northern maritime climates.

Acknowledgements

The work described in this paper was funded by the Higher Education Authority of Ireland Technological Sector Strand III and the Arnold F. Graves grants. Support from Dr. M. Mc Keever in setting up the automated control system is highly appreciated.

Nomenclature

A_c collector area (m^2)
C_p specific heat capacity of solar fluid (J/kg/K)
E_i daily solar energy input ($MJ/m^2/d$)
E_c daily energy collected ($MJ/m^2/d$)
G_t total global solar radiation on the collector's surface (W/m^2)
$\dot{m}$ solar fluid mass flow rate (kg/s)
Q_{aux} auxiliary heating requirement (MJ)
Q_c useful heat collected (J)
Q_d useful heat delivered (J)
Q_l supply pipe heat loss (J)
Q_s solar yield (MJ)
SF solar fraction (%)
η_c collector efficiency (%)
η_s system efficiency (%)

References

[1] S.A. Kalogirou, Solar thermal collectors and applications, Progress in Energy and Combustion Science, 30 (3) (2004) 231-295.

[2] The German Solar Energy Society, Planning and installing solar thermal systems: A guide for installers, architects and engineers, James and James, UK, 2007.

[3] L.M. Ayompe, A. Duffy, S.J. McCormack, M. Conlon, Validated TRNSYS model for forced circulation solar water heating systems with flat plate and heat pipe evacuated tube collectors, Applied Thermal Engineering, 31 (8–9) (2011) 1536-1542.

[4] European Standards, CSN EN 12975-2 - Thermal solar systems and components - Solar collectors - Part 1: General requirements, (2006)

[5] ASHRAE-93, Methods of Testing to Determine the Thermal Performance of Solar Collectors, ASHRAE, Atlanta, 2003.

[6] E. Zambolin, D. Del Col, Experimental analysis of thermal performance of flat plate and evacuated tube solar collectors in stationary standard and daily conditions, Solar Energy, 84 (8) (2010) 1382-1396.

[7] R.C. Tiwari, A. Kumar, S.K. Gupta, G.D. Sootha, Thermal performance of flat-plate solar collectors manufactured in India, Energy Conversion and Management, 31 (4) (1991) 309-313.

[8] E.H. Amer, J.K. Nayak, G.K. Sharma, Transient method for testing flat-plate solar collectors, Energy Conversion and Management, 39 (7) (1998) 549-558.

[9] Z. Chen, S. Furbo, B. Perers, J. Fan, E. Andersen, Efficiencies of flat plate solar collectors at different flow rates, Energy Procedia, 30 (0) (2012) 65-72.

[10] A. Sakhrieh, A. Al-Ghandoor, Experimental investigation of the performance of five types of solar collectors, Energy Conversion and Management, 65 (0) (2013) 715-720.

[11] M.C. Rodríguez-Hidalgo, P.A. Rodríguez-Aumente, A. Lecuona, J. Nogueira, Instantaneous performance of solar collectors for domestic hot water, heating and cooling applications, Energy and Buildings, 45 (0) (2012) 152-160.

[12] I.M. Michaelides, P.C. Eleftheriou, An experimental investigation of the performance boundaries of a solar water heating system, Experimental Thermal and Fluid Science, 35 (6) (2011) 1002-1009.
[13] L.M. Ayompe, A. Duffy, M. Mc Keever, M. Conlon, S.J. McCormack, Comparative field performance study of flat plate and heat pipe evacuated tube collectors (ETCs) for domestic water heating systems in a temperate climate, Energy, 36 (5) (2011) 3370-3378.
[14] Building Research Establishment, 2009. Clearline Solar Thermal Test Report – Average Household Simulation, Viridian Solar, Client report number 251175, 2009. Available at: http://www.viridiansolar.co.uk/Assets/Files/BRE_Report_Viridian_Solar_Average_House_Simulation.pdf.
[15] European Commission, Mandate to CEN and CENELEC for the elaboration and adoption of measurement standards for household appliances: water heaters, hot water storage appliances and water heating systems, Brussels, 2002.
[16] S.A. Kalogirou, Solar energy engineering: Processes and systems, Elsevier, London, 2009.
[17] S.P. Sukhatme, Solar energy: Principles of thermal collection and storage, 2nd ed., Tata McGraw-Hill, New Delhi, 1998.
[18] J.A. Duffie, W.A. Beckman, Solar engineering of thermal processes, Wiley, New York, 2006.
[19] E. Mathioulakis, G. Panaras, V. Belessiotis, Uncertainty in estimating the performance of solar thermal systems, Solar Energy, 86 (11) (2012) 3450-3459.
[20] S. Bell, A beginner's guide to uncertainty of measurement, Measurement Good Practice Guide No. 11 (Issue 2 with amendments), 2001, National Physical Laboratory, Middlesex, UK.